Research Article GU J Sci 37(4): 1964-1979 (2024) DOI: 10.35378/gujs.1390096

Gazi University

Journal of Science

http://dergipark.gov.tr/gujs

Investigation of Microstructures and Mechanical Properties of Al2024/6061/7075-Graphene Composites

Elif ISIK[1], Mahmut Can SENEL[2,*], Aleyna TASKIN[2]

[1]*Sivas University of Science and Technology, Department of Metallurgical and Materials Engineering, 58100, Sivas, Türkiye*
[2]*Ondokuz Mayıs University, Department of Mechanical Engineering, 55210, Samsun, Türkiye*

Highlights

- A new heat-treatment method was used for manufacturing Al2024/6061/7075-based composites.
- The induction hot-pressing technique is an impressive method for enhancing the mechanical properties.
- The effect of graphene content and matrix material on microstructures of composites was focused.

Article Info

Received: 13 Nov 2023
Accepted: 21 Mar 2024

Keywords

Aluminum
Graphene
Powder Metallurgy
Microstructure
Strength

Abstract

This work aimed to compare the mechanical properties and microstructures of Al2024-graphene, Al6061-graphene, and Al7075-graphene composites produced via the induction hot pressing and powder metallurgy method. The influences of graphene content (0.15-0.45wt.%), heat treatment (sintering and induction hot-pressing), and matrix material (Al2024, Al6061, and Al7075) on the mechanical strength and microstructure of specimens were studied. Compared to Al2024, Al6061 and Al7075 alloys, the compressive strength of Al2024-0.15graphene, Al6061-0.15graphene and Al7075-0.15graphene composites increased by 33.74%, 24.9% and 32%, respectively. The highest compressive strength (506±5 MPa), hardness (164±1.5 HV), and apparent density (2.65 g/cm^3) were achieved in sintered and induction heat-treated Al7075-0.15%graphene composite. As a result, it was determined that graphene is an effective reinforcement element. It has been determined that induction hot-pressing improves the mechanical strength of composite materials.

1. INTRODUCTION

Developments in science and technology have led to the emergence of special needs, especially in the fields of materials. This situation has led to the fact that traditional materials, which have begun to be inadequate in the sector, are replaced by advanced technology materials with superior properties. For this purpose, ongoing studies have been focusing on composite materials, particularly in recent years. These studies, which are carried out with combinations of different types of materials and production methods, are critical in terms of literature [1].

Composite materials are formed by combination of at least two materials to obtain a material with superior properties. Composite materials show the properties of all the materials that make up the structure [2]. Among these materials, metal matrix composite materials are frequently used due to their properties such as corrosion resistance, high specific strength, hardness, and wear [3].

The main element of metal matrix composites (MMCs) consists of metals such as titanium (Ti), nickel (Ni), copper (Cu), aluminum (Al), magnesium (Mg), iron (Fe), and their alloys [4]. In particular, aluminum and its alloys, which are distinguished from other materials with their properties such as lightness, high strength, elasticity modulus, and low thermal coefficient, are often utilized as main elements in MMCs [5]. In addition, aluminum attracts attention because of its easy formability, low cost, and recyclability [6]. In this work, Al2024, Al6061, and Al7075 alloys were preferred as matrix materials. The main alloying element of Al2024 aluminum alloy is copper. It is generally used in the aerospace and automotive industries because

*Corresponding author, e-mail: mahmutcan.senel@omu.edu.tr

of its high fracture toughness, high fatigue strength, and easy formability [7, 8]. The primary alloying elements of Al6061 aluminum alloy are magnesium and silicon. Al6061 aluminum alloys have advantages such as high corrosion resistance, easy machinability, and weldability [9]. Al7075 alloy stands out among aluminum alloys with properties such as high fracture toughness, high lightness, and strength. Al7075 aluminum alloy, the primary alloying element of which is zinc, is often preferred in aerospace and automotive applications [10]. In metal matrix composite materials, aluminum oxide (Al_2O_3) [11], zirconium dioxide (ZrO_2) [12], titanium dioxide (TiO_2) [13], boron carbide (B_4C) [14], titanium carbide (TiC) [15], silicon carbide (SiC) [16], silicon nitride (Si_3N_4) [17], boron nitride (BN) [18], graphene nanoplatelets (GNPs) [19], carbon nanotube (CNT) [20] and graphite [21] are frequently used as reinforcing elements. Graphene consists of carbon atoms with a covalent bond between them and is arranged in a honeycomb form which is included in these materials. GNPs offer an excellent combination of mechanical, electronic, optical, thermal, and electrochemical properties which have a layered and two-dimensional structure [22]. Graphene attracts attention among researchers and is the subject of many academic studies which is a promising material thanks to its extraordinary properties. Graphene has gained a place in many sectors, especially in electrical-electronics, biomedical, food, and automotive. Applications of graphene in these fields include sensors, transistors, semiconductors, lithium-ion batteries, fuel cells, electronic devices, coatings, etc. [23].

Stir casting [24], powder metallurgy (PM) [25] squeeze casting [26], and friction stir [27] are used to produce composite material with the metal matrix. Among these methods, the PM method, which enables the production of small and complex shaped parts with high precision, is among the most preferred methods in the fabrication of MMCs [28]. The use of traditional sintering methods in the production of MMCs by powder metallurgy causes grain growth in the specimens because of the application of high temperatures for a long time. In addition, these methods cause significant energy costs. To prevent such problems, various sintering techniques (hot pressing, spark plasma, induction heat treatment, etc.) have been developed. One of these methods is induction hot pressing, in which temperature and pressure are applied together. The effect of the high pressure and temperature causes the grains to come closer together, thus, porosity is decreased and grain growth is prevented. In the induction hot pressing process, a magnetic field is created on the material using an induction coil. Heat is released due to the power loss caused by metal resistance in the material within the magnetic field. The sample can reach the desired temperature in a very short time due to the heat. In addition, any deformation, such as oxidation, does not occur on the material surface since the process happens quickly. For this reason, the induction hot pressing method is preferred in many studies to enhance the mechanical strength of MMCs [29, 30].

When the literature was examined, there were many studies on the fabrication of Al-based composites and the examination of their microstructures and mechanical properties. Chen et al. [31] carried out the production of graphene-reinforced (0.5, 0.8, 1, 1.5 wt.%) Al2024-based composite using the PM method. As a consequence of tests, optimum values were reached in Al2024-1%GNPs composites. The hardness and strength of the composites increased by 5.7% and 41.6%, respectively. Singh [32] explained the mechanical strength of Al2024-xGNPs (x=0.5-4wt.%) produced by the stir casting method. The highest values were reached in samples with 3% graphene by weight. AbuShanaba et al. [33] reported the effect of graphene reinforcement in different ratios (0, 0.25, 0.5, 1, 2wt.%) on the microstructure and mechanical strength of the Al2024-GNPs composite. The specimens were heat-treated at 460°C and 560°C. It was stated that the rise in graphene reinforcement increased the mechanical strength and optimum values were reached in sintered Al2024-2%GNPs composites at a 560°C sintering temperature. Kumar and Xavior [34] produced Al6061-GNPs composites containing graphene in the proportions of 0.2, 0.4, 0.6, and 0.8wt.% by the powder metallurgy method. Based on the mechanical tests, the highest hardness (64 HV) and flexural strength (89 MPa) were achieved in the Al-0.4%GNPs composite. Khan et al. [35] produced Al6061-GNPs composites (GNPs: 0.1, 0.5, 1, 3 wt%). Powder metallurgy was preferred as the production method. Compressive strength, hardness, and flexural strength of 1wt.% graphene-reinforced Al-based composite increased by ~61%, ~93%, and ~92%, respectively. Chak and Chattopadhyay [36] examined the mechanical properties of Al7075-GNPs samples containing various reinforcement ratios of graphene (0.1-0.5wt.%) synthesized by the stir casting technique. Based on the results of mechanical tests, maximum hardness value was observed in Al7075-0.5%GNPs and the highest tensile strength value was reached in 0.3%GNPs reinforced Al7075-based composite. Compared to base material, the tensile strength and the

hardness values have improved by ~53.39%, and ~56.55% respectively. Xia et al. [37] researched the effects of GNPs amount on the mechanical properties of Al7075 matrix composites. GNP reinforcement significantly enhanced the mechanical performance of the specimens. Hardness and elastic modulus exhibited remarkable improvements, with increases of approximately 29% and 36%, respectively. Darshan et al. [24] researched the mechanical strength of Al7075-0.6%GNPs produced via the hot extrusion and powder metallurgy methods. Consequently, based on the microstructural investigations, it was found that GNPs were uniformly distributed in the microstructure. Moreover, it was revealed that graphene reinforcement increased the tensile stress and hardness values by ~42.93% and ~43.54%, respectively.

Previous studies in this area of research have reported in which Al2024-GNPs, Al6061-GNPs, and Al7075-GNPs composites are fabricated, and their mechanical properties and microstructure are analyzed. However, a study was not found to compare graphene-reinforced composites with the Al2024, Al6061 and Al7075 matrix. Furthermore, there is no study of the application of post-sintering heat treatment and the mechanical strength of composites from this process. For this purpose, the microstructure and mechanical properties of Al2024-GNPs, Al6061-GNPs, and Al7075-GNPs composites fabricated by hot pressing and powder metallurgy methods were compared. This comparison study aims to provide a better understanding of the interaction of Al2024, Al6061, and Al7075 aluminum alloys with graphene and the properties of different aluminum alloys. Furthermore, the effects of graphene reinforcement ratio, matrix material type, and induction heat treatment on the mechanical strength and microstructure of composites were researched.

2. MATERIAL METHOD

2.1. Material

In the present work, Al2024, Al6061, and Al7075 alloys were preferred as matrix materials, while graphene (0.15, 0.30, and 0.45wt.%) was selected as the reinforcing element. All of the aluminum alloy powders used in the study were obtained from Nanografi Technology (Turkey) and the chemical compositions of aluminum alloy powders were given in Table 1. Al2024, Al6061, and Al7075 aluminum alloy powders have a theoretical density of approximately 2.78 g/cm^3, 2.70 g/cm^3, and 2.81 g/cm^3, and a powder size of ~10 μm, respectively. Graphene nanoplatelets were preferred as a reinforcement element which was supplied by Graphene Chemical Industry (Türkiye), had a theoretical density of 2.25 g/cm^3, a diameter of 5-10 μm and a thickness of 5-8 nm.

Table 1. *The chemical compositions of Al2024, Al6061 and Al7075 alloys (wt%)*

Material	Al	Cu	Mg	Si	Zn	Fe	Mn	Cr	Ti
Al2024	90.9	4.9	1.8	0.5	0.25	0.5	0.9	0.1	0.15
Al6061	96	0.4	1.2	0.8	0.25	0.7	0.15	0.35	0.15
Al7075	90.02	1.2	2.1	0.4	5.1	0.5	0.3	0.18	0.2

SEM photographs of Al2024, Al6061, Al7075 alloys, and graphene powders are given in Figure 1. Al2024, Al6061, and Al7075 aluminum alloy powders are given in Figure 1(a-c). These powders have an irregular shape which is a particle size of ~10 μm. SEM images of graphene powders are provided in Figure 1(d). It shows that graphene powders are two-dimensional, layered, and irregularly shaped powders. In addition, it is seen that the graphene layers have a thickness of fewer than 100 nm.

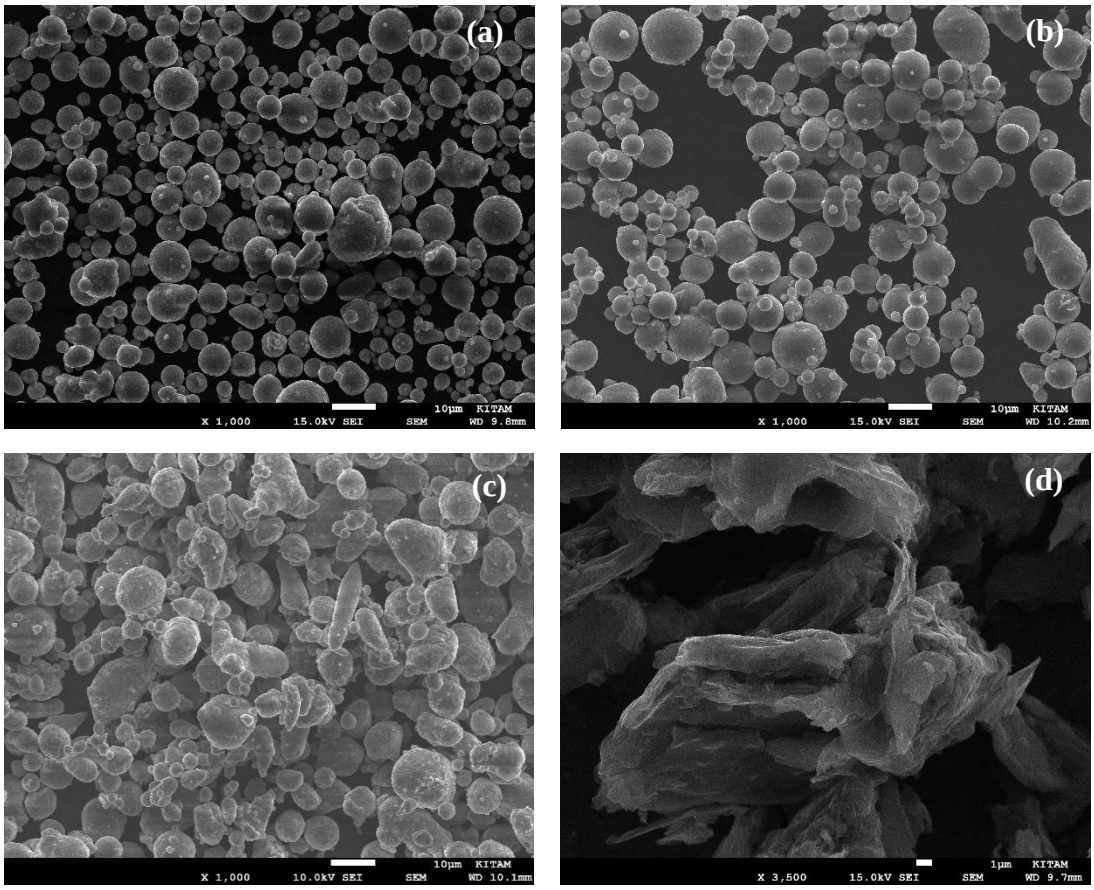

Figure 1. *SEM pictures of powders: (a) Al2024, (b) Al6061, (c) Al7075 alloy, and (d) graphene*

2.2. Method

2.2.1. Preparing samples

In this study, Al2024-GNPs, Al6061-GNPs, and Al7075-GNPs composites were fabricated using hot pressing and PM method. The schematic illustration of the manufacturing process is given in Figure 2. In the first step of the production process, aluminum alloy powder (Al2024/Al6061/Al7075) and ethanol were mixed for 1 h via a mechanical mixer. Meanwhile, graphene was distributed in ethanol via a high-energy ball milling. Then, the aluminum alloy-ethanol mixture was slowly added to the graphene-ethanol mixture. The mixing process was carried out in a ball milling and hence, the mixture could be stirred homogeneously. After mixing, the prepared powders were filtered and dried under a continuous vacuum for 16 hours at 50°C. Mixed powders were pressed in a die with the help of a uniaxial press under 700 MPa pressure. The formed specimens were sintered at 600 °C for 1 hour under a continuous vacuum. After the sintering process, hot-pressing was applied to increase the density and properties of the mechanical of the samples. The induction heating machine was used in this process which has an output power of 2-15 kW, an output current of 0-34 A, and a frequency of 50 Hz. A single-axis hydraulic press (10 tons load capacity) is also integrated into the induction heating machine for the hot-pressing process. During this process, the samples placed in the graphite die (13.5x13.5 mm) were pressed under 25 MPa pressure by raising them to a temperature of 500°C in 41 seconds. A copper induction coil with a 4 mm diameter and 0.5 mm wall thickness was used for heating. After holding (30 s) and cooling (10 s) steps, the samples were removed from the die. Finally, the samples were sanded (600, 1200, and 2500 grit) and polished with a 1 μm diamond paste to prepare them for microstructure analysis and mechanical tests.

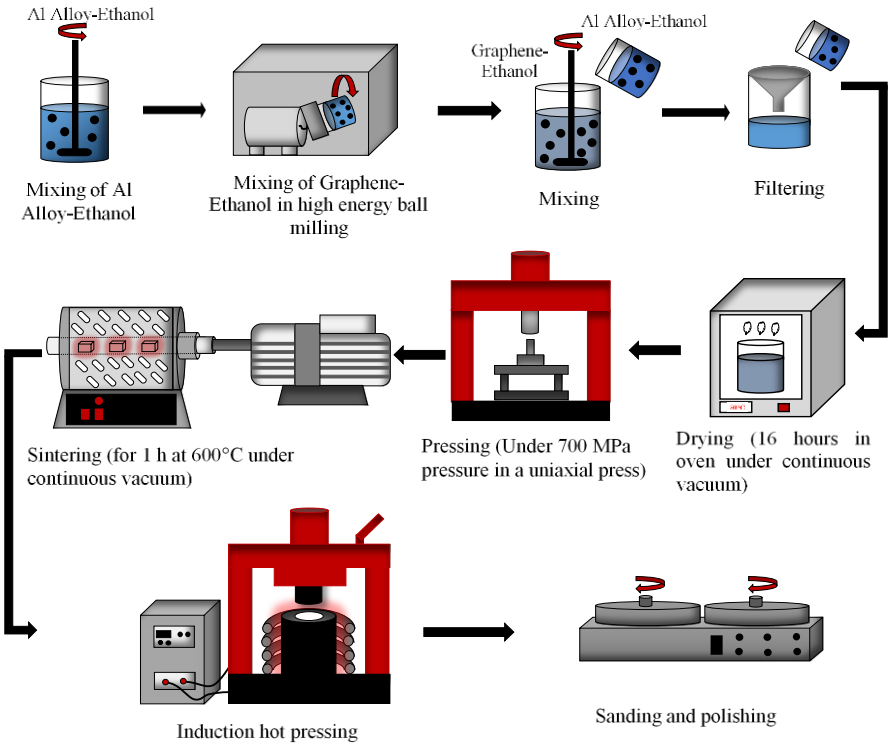

Figure 2. *Schematic illustration of the manufacturing process*

2.2.2. Mechanical and physical tests

The hardness, density, and compression tests of the Al2024-GNPs, Al6061-GNPs, and Al7075-GNPs composite samples were performed in this paper. In addition, the physical and mechanical properties of samples were examined for different heat treatment and graphene content. Archimedes method was applied for density determination of the specimens. The density results were calculated by averaging five different measurements. The experimental densities (ρ_D) of the composites may be detected by Equation (1) [38]

$$\rho_D = \rho_W \times [m_K \times (m_D - m_A)^{-1}] \ . \quad (1)$$

In this equation, ρ_W represents the density of water, while m_K, m_D, and m_A represent the dry mass of the specimen, the suspended mass of the specimen in water, and the mass of the saturated specimen, respectively. The theoretical density (ρ_T) of the produced samples can be calculated as below taking into account the mass fraction of aluminum alloys (ρ_{Al2024} = 2.78 g/cm^3, ρ_{Al6061} = 2.7 g/cm^3, ρ_{Al7075} = 2.81 g/cm^3) and graphene (ρ_{GNPs} = 2.25 g/cm^3) [38]

$$\rho_T = (m_{Al}\% \times \rho_{Al}) + (m_{GNPs}\% \times \rho_{GNPs}) \ , \quad (2)$$

where m_{Al} and m_{GNPs} are the mass fractions of aluminum alloy and graphene, respectively. The relative density is calculated as the ratio of the density of the samples to their theoretical density. This value is used to detect the porosity rate (P%) of the samples. The porosity rate can be calculated by Equation (3) [38]

$$P\% = (1 - \rho_D/\rho_T) \times 100 \ . \quad (3)$$

Micro Vickers hardness tests were preferred for hardness measurements. During the hardness test, a force of 200 gf was applied on the polished sample surface for 15 seconds. Hardness was determined by averaging five measurements taken across the sample surface. The strength of the samples (11.5×11.5×4.5 mm) was determined by compression test (ASTM E9) at a compression speed of 3 mm/min. This strength was detected by averaging the results of three compression tests.

2.2.3. Characterization

The microstructures of the prepared specimens and powders were analyzed using SEM device. Beside this, Energy Dispersive X-ray (EDX) examinations were performed to reveal the dispersion of graphene powders. The phase investigation of powders and produced specimens were analyzed using X-ray diffraction analysis (XRD). The XRD analyses were carried out in the scanning angle range of 20° and 80° at a 0.02° scanning rate at a 0.154 nm wavelength with Cu-Kα radiation.

3. THE RESEARCH FINDINGS AND DISCUSSION

3.1. XRD and Fracture Surface Analysis

XRD analyses were performed to determine the phase structures of the powders and the samples. Figure 3 shows XRD patterns of Al2024, Al6061, Al7075 aluminum alloys, Al2024-GNPs, Al6061-GNPs, and Al7075-GNPs composites. These graphs showed that the diffraction angles (2Θ = ~38.8º, 45.2º, 65.3º, and 77.8º) of aluminum alloys (Al2024, Al6061, and Al7075) were the same for all composites. The graphene peak (2θ = ~26.8º) was not detected due to the low graphene reinforcement ratio and the limited sensitivity of the XRD device. Moreover, the sintering and hot-pressing processes did not result in any phase transformations or undesired secondary phase formation such as Al_4C_3 in the graphene-reinforced aluminum-based composites.

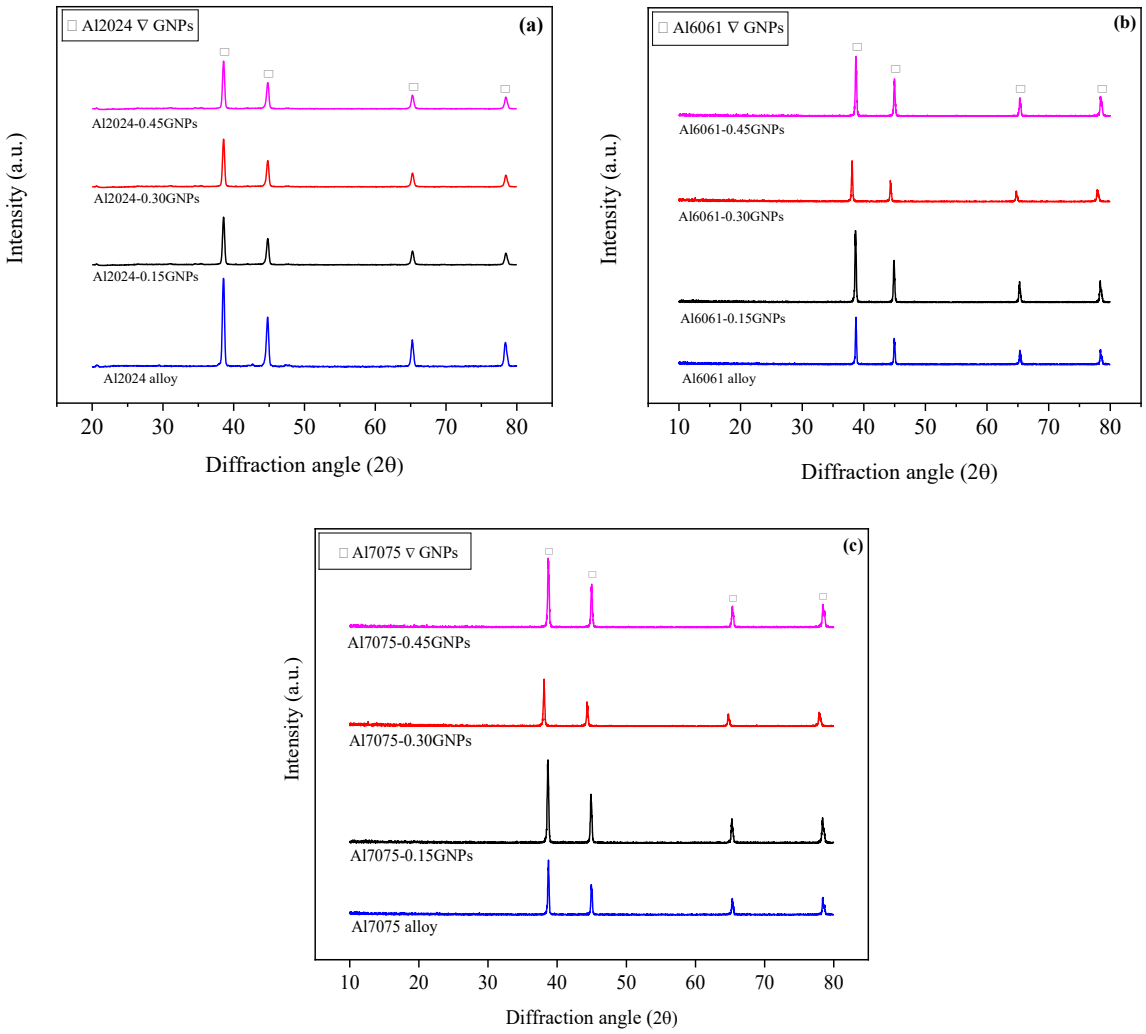

Figure 3. *X-Ray diffraction plots of prepared samples: (a) Al2024-GNPs, (b) Al6061-GNPs, and (c) Al7075-GNPs composites*

Figure 4 (a-i) illustrates fracture surface SEM images of hot-pressed and sintered Al2024-GNPs, Al6061-GNPs, and Al7075-GNPs composites. When SEM images were evaluated, it was determined that the graphene particles in Al2024-0.15%GNPs, Al6061-0.15%GNPs, and Al7075-0.15%GNPs composites were homogeneously dispersed and located the grain boundaries. Graphene particles at the grain boundaries prevented grain growth during the thermal processes. Also, the particles are refined to fine grains without any coarsening. Furthermore, an increase in the interaction between the grains was observed. Consequently, it resulted in a denser microstructure and led to an improvement in the strength of the specimen. This phenomenon could be described by the grain refinement strengthening phenomenon. On the other hand, clumped graphene nanoplatelets were determined in composites containing 0.45wt%graphene as presented in Figure 4(c), (f), and (i). Clumping graphene weakened the interfacial bonding among the particles. It caused the formation of pores in the microstructure. It can be described by the decrease in physical and mechanical properties of the produced specimens after 0.15wt.%GNPs amount.

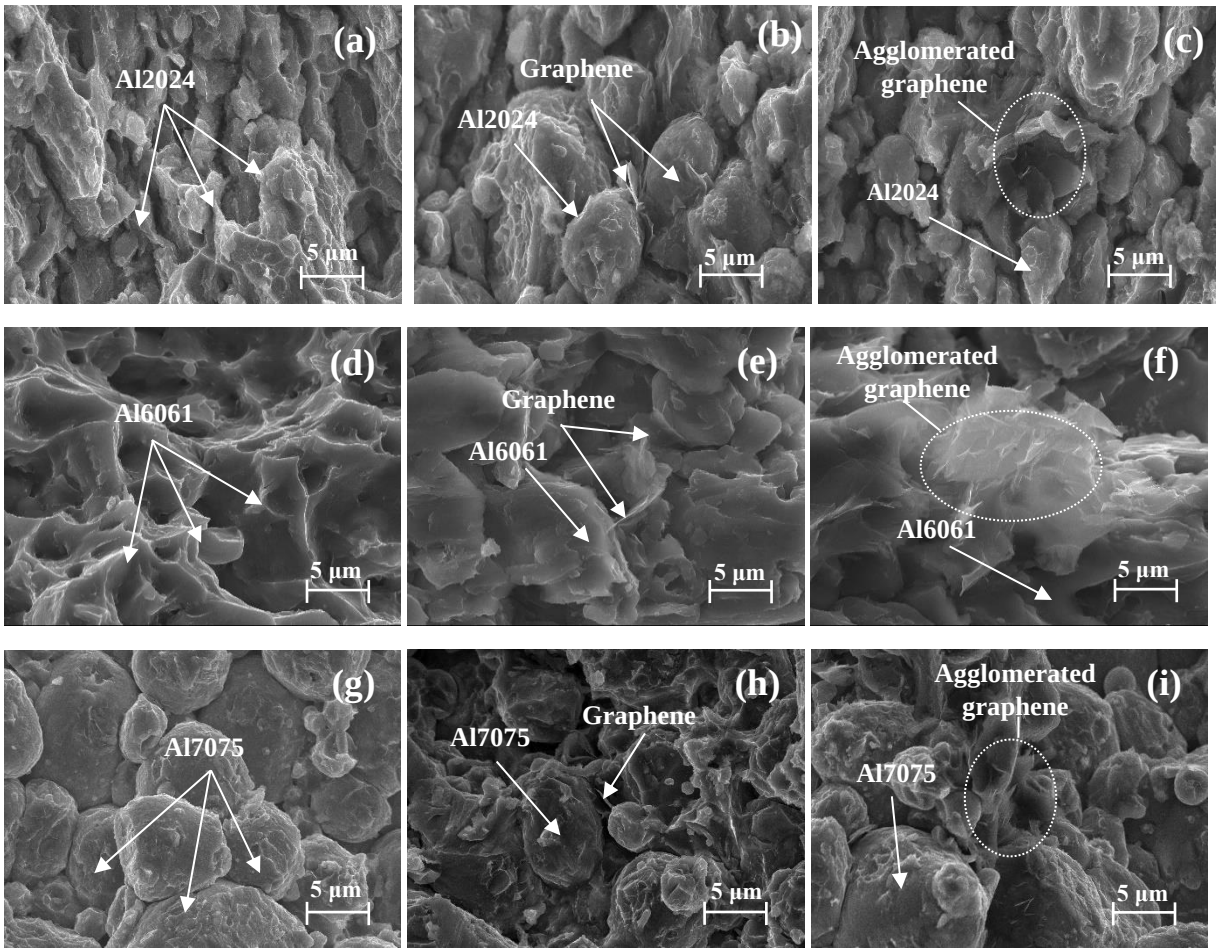

Figure 4. *Fractured surface SEM pictures for induction heat-treated and sintered samples: (a) Al2024, (b) Al2024-0.15GNPs, (c) Al2024-0.45GNPs, (d) Al6061, (e) Al6061-0.15GNPs, (f) Al6061-0.45GNPs, (g) Al7075, (h) Al7075-0.15GNPs, and (i) Al7075-0.45GNPs composites*

Images of SEM-EDX and element distributions of Al2024-0.45%GNPs, Al6061-0.45%GNPs, and Al7075-0.45%GNPs samples are given in Figure 5. Considering the element distribution of Al2024-0.45%GNPs (Figure 5(a)), the green and turquoise blue colors represent the Al and C distributions in the microstructure. The high intensity of carbon elements indicated the agglomerated graphene nanoplatelets. As seen from the SEM-EDX images of Al6061-0.45%GNPs composites (Figure 5(b)), green and red colors show the distribution of Al and graphene, respectively. Similarly, it was seen that high graphene content in the microstructure prevented the homogenous distribution of graphene. When element distribution maps of the Al7075-0.45%GNPs composites (Figure 5(c)) were investigated, green and red colors represent the distribution of Al and graphene, respectively. Based on the SEM-EDX maps of the composites, the distribution of carbon elements confirmed the absence of graphene in the microstructure. These element

distribution maps also revealed that graphene particles located at the grain boundaries. Apart from this, agglomerations were detected in all composites containing 0.45wt.%graphene. The stacked and clustered graphene nanoplatelets in SEM-EDX images were determined around the Al grains due to the nanosized structure of graphene. The clumping of the graphene particles led to a decrease in the bond strength between the grains. This ultimately resulted in weaker composites due to reduced resistance to graphene sliding during the pressing process.

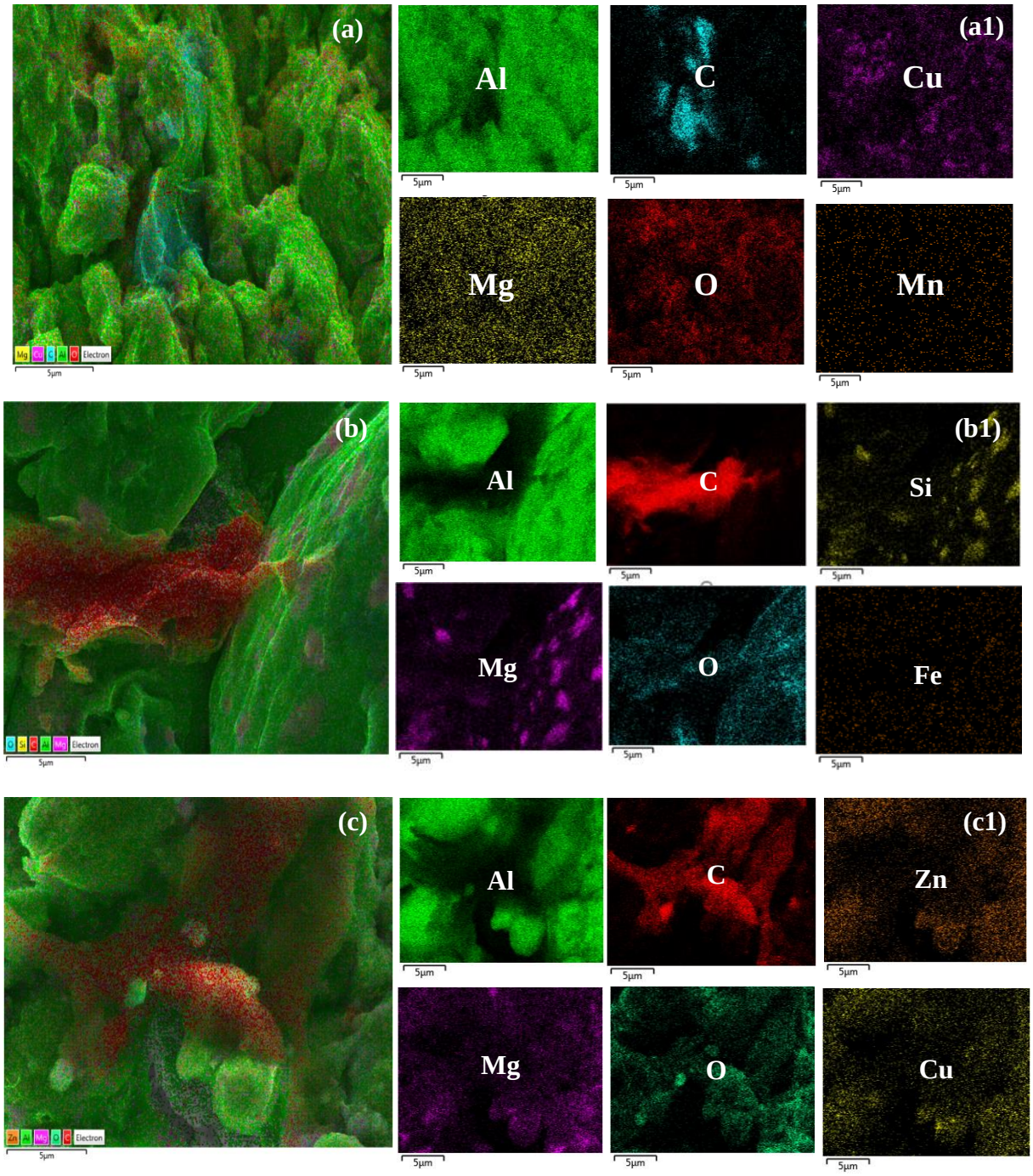

Figure 5. *Images of SEM-EDX mapping and element distributions for induction heat-treated and sintered composites: (a, a1) Al2024-0.45GNPs, (b, b1) Al6061-0.45GNPs, and (c, c1) Al7075-0.45GNPs composites*

3.2. Density And Hardness Test Results

Table 2 displays the effect of graphene quantity and heat treatment process on the density and porosity ratio of Al2024-GNPs, Al6061-GNPs, and Al7075-GNPs composites. The data showed that the graphene addition enhanced the density of Al2024 alloy from 2.58 g/cm^3 to 2.62 g/cm^3 (Al2024-0.15%GNPs), which further increased to 2.65 g/cm^3 after hot pressing. When the porosity rate was examined, the lowest porosity rate of 4.6% was reached in the Al2024-0.15%GNPs composite. Considering Al6061-GNPs composites, the porosity rate and density improved from 4.8%, 2.56 g/cm^3 (Al6061 alloy) to 4.4%, 2.58 g/cm^3 (Al6061-0.15%GNPs) with the GNPs addition. When the variation of density and porosity ratio of Al7075-GNPs composites was evaluated, it was found that the maximum density (2.65 g/cm^3) and the minimum porosity ratio (5.4%) were reached in hot-pressed and sintered Al7075-0.15%GNPs composite. As a result, the hot-pressed and sintered Al2024-0.15%GNPs and Al7075-0.15%GNPs composites exhibited the maximum density (2.65 g/cm^3). Otherwise, the lowest porosity rate (4.4%) was determined in the Al6061-0.15%GNPs composite. Graphene distribution in the microstructure is a parameter that directly affects the density and porosity rate. As a result of the microstructure examinations in the study, the most homogeneous graphene distribution was observed in Al6061-GNPs composites. Hence, a lower porosity rate was obtained in Al6061-GNPs composites compared to Al2024-GNPs and Al7075-GNPs composites. Due to the deformation effect after hot pressing, the microstructure was densified and the porosity rate decreased thanks to the convergence of the grains. On the other hand, a reduction in density and an increase in porosity rate were recorded above 0.15wt.% graphene content. It could be caused by the agglomeration of graphene particles. The increased porosity rate could result in a weaker material with lower strength and hardness.

Table 2. *Apparent density, porosity ratio and % apparent density values for Al2024-GNPs, Al6061-GNPs and Al7075-GNPs composites*

Specimen	Apparent Density (g/cm^3)		%Apparent Density		%Porosity	
	Sintered	Sintered and induction hot-pressed	Sintered	Sintered and induction hot-pressed	Sintered	Sintered and induction hot-pressed
Al2024	2.58	2.63	92.8	94.6	7.2	5.4
Al2024-0.15%GNPs	2.62	2.65	94.3	95.4	5.7	4.6
Al2024-0.30%GNPs	2.57	2.59	92.5	93.2	7.5	6.8
Al2024-0.45%GNPs	2.55	2.57	91.8	92.5	8.2	7.5
Al6061	2.55	2.56	94.4	95.2	5.6	4.8
Al6061-0.15%GNPs	2.57	2.58	95.2	95.6	4.8	4.4
Al6061-0.30%GNPs	2.53	2.52	93.8	94.5	6.2	5.5
Al6061-0.45%GNPs	2.51	2.50	93.1	93.4	6.9	6.6
Al7075	2.60	2.62	92.9	93.6	7.1	6.4
Al7075-0.15%GNPs	2.63	2.65	93.9	94.6	6.1	5.4
Al7075-0.30%GNPs	2.61	2.62	93.1	93.5	6.9	6.5
Al7075-0.45%GNPs	2.57	2.58	91.7	92.1	8.3	7.9

The Vickers hardness results for Al2024-GNPs, Al6061-GNPs, and Al7075-GNPs composite materials are given in Figure 6. The highest hardness value (100.3±1.5 HV) was determined in sintered and hot-pressed Al2024-0.15%GNPs composite among Al2024-based composites (Figure 6(a)). The hardness value improved from 94.8±1.2 HV to 100.3±1.5 HV. In Figure 6(b), the hardness value improved from 108±2 HV (Al6061 alloy) to 151±1 HV (Al6061-0.15%GNPs) with hot-pressing and sintering process. When the hardness variation of Al7075-GNPs composites was examined, the highest hardness value (164±1.5 HV) was reached in Al7075-0.15%GNPs composites (Figure 6(c)). The hardness value increased from 128±2 HV (Al7075 alloy) to 164±1.5 HV (Al7075-0.15%GNPs) with the sintering and hot-pressing process. As shown in Figure 6, the hardness value of the sintered and hot-pressed samples was observed to be higher than that of only sintered samples for the same composition. The highest increase rate (~37%) in hardness was found in Al6061-0.15%GNPs composites. With the effect of hot pressing, the grains undergo hot deformation and come close to each other. The grains come close to each other causing a rise in the

hardness of the composite due to the mechanism of grain refinement. Moreover, the high surface area of GNPs further enhanced the composite's hardness [2]. However, a decrease in hardness was observed after 0.15wt.% graphene reinforcement rate. This situation is caused by the clumping behavior in the microstructure due to the electrostatic attraction among the nano-size particles of graphene.

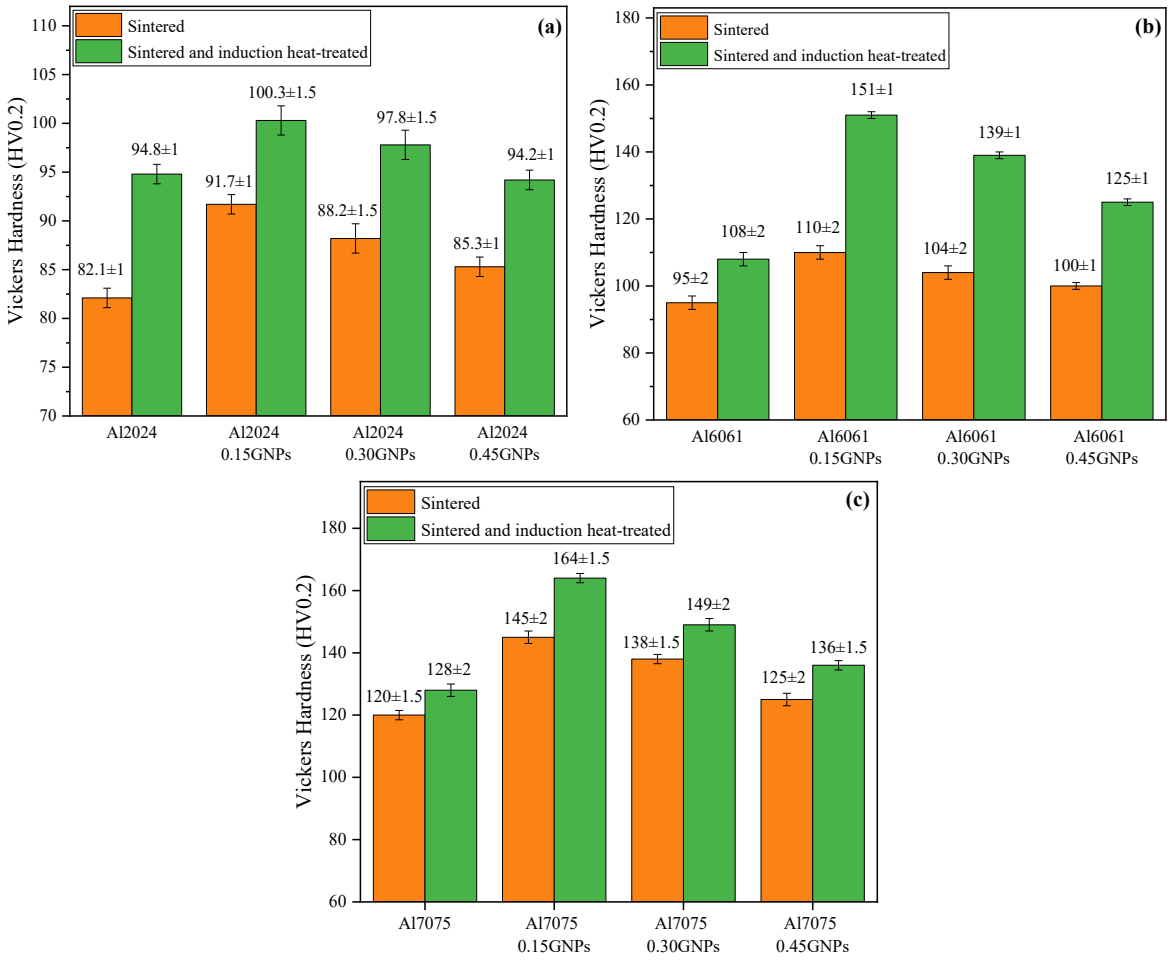

Figure 6. *The variation of Vickers hardness for various graphene content and heat treatment process: (a) Al2024-GNPs, (b) Al6061-GNPs, and (c) Al7075-GNPs composites*

3.3. Compressive Strength Test Results

Figure 7 shows the compressive strength results of Al2024-GNPs, Al6061-GNPs, and Al7075-GNPs composites. According to the results, the highest compressive strength values were determined in sintered and hot-pressed Al Alloy-0.15GNPs composites. As presented in Figure 7(a), the compressive strength of the Al2024-0.15GNPs composites increased from 325±4 MPa to 453±4 MPa because of the hot-pressing operation. When the compressive strength of Al6061-GNPs was examined (Figure 7(b)), the strength increased from 273±5 MPa (Al6061 alloy) to 341±6 MPa (Al6061-0.15GNPs) for the only sintering process. It was seen that this value raised to 484±6 MPa (Al6061-0.15GNPs) for the hot-pressing process. Figure 7(c) shows that the highest compressive strength was obtained as 506±6 MPa for the hot-pressed and sintered Al7075-0.15%GNPs. In summary, the compressive strength increased with graphene reinforcement for all matrix materials. Because graphene nanoplatelets carry a significant part of the load. This phenomenon is called the load transfer mechanism. On the other hand, compressive strength decreased sharply at the content above 0.15wt.% graphene. The decrease in compressive strength is because of the weakening of the interfacial bond between the aluminum alloy and GNPs due to agglomerated graphene particles in the microstructure. The results demonstrated that the hot pressing process enhances the compressive strength of the specimens. Since the hot-pressing operation is applied at high temperatures, it leads to the strengthening of the bond between the grains and the formation of necks between the grains.

This also caused the compressive strength to improve. The highest compressive strength (506±6 MPa) was determined at hot-pressed and sintered Al7075-0.15%GNPs. This is due to the fact that Al7075 is a more effective matrix material. Also, it is thought that Al7075 and graphene have better interface interactions than other composites.

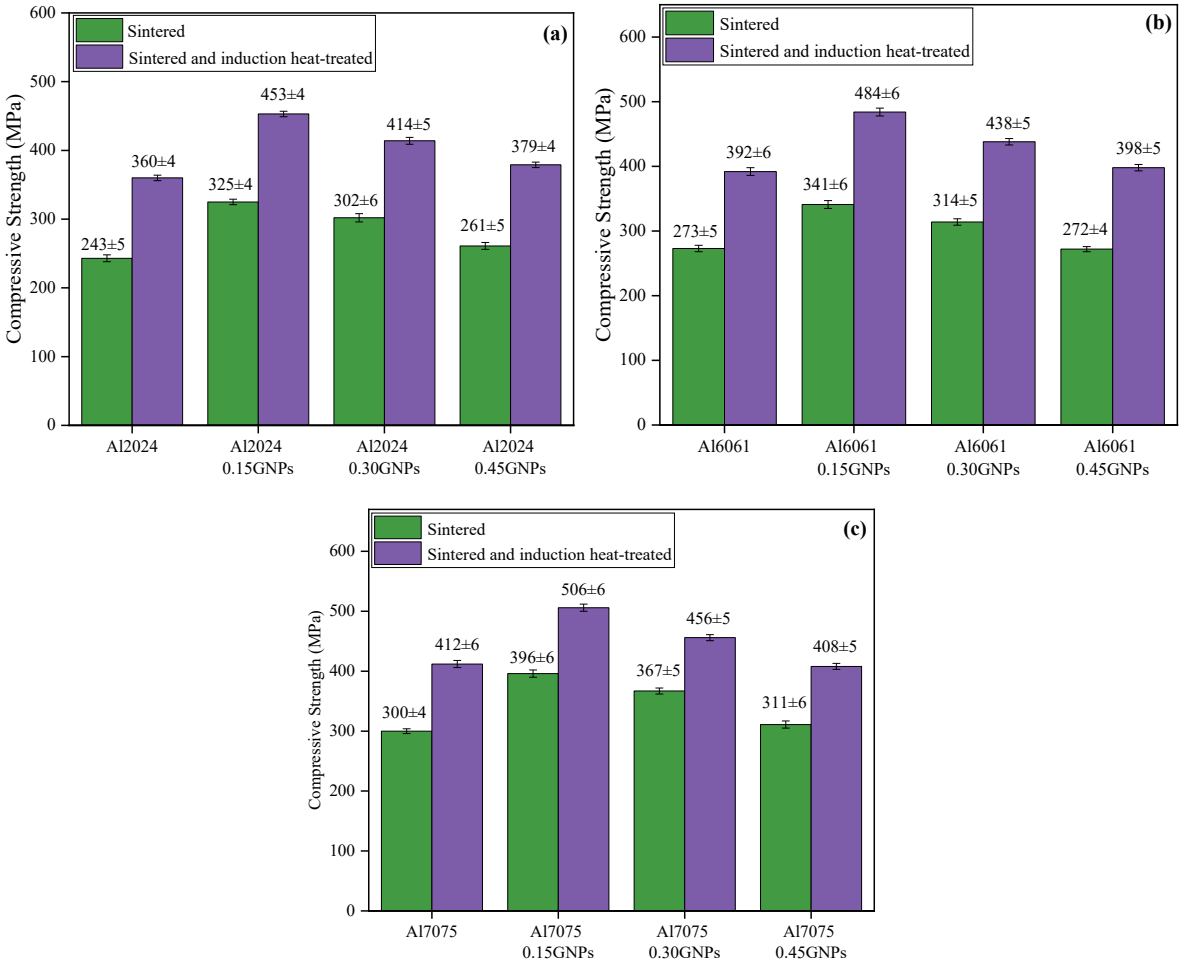

Figure 7. *The variation of compressive strength for various graphene content and heat treatment process: (a) Al2024-GNPs, (b) Al6061-GNPs, and (c) Al7075-GNPs composite*

Some strengthening phenomena can explain the effect of reinforcements on the strength of the composites based on aluminum. Considering Al-GNPs composites, the most commonly used strengthening mechanisms are load transfer mechanism ($\Delta\sigma_{LT}$), fine grain reinforcement ($\Delta\sigma_{GR}$), thermal mismatch strengthening ($\Delta\sigma_{CTE}$), and Orowan cycle ($\Delta\sigma_{OR}$) [39, 40]. The total influence of each of these mechanisms on the strength of yield can be defined by Equation (4) [41]

$$\Delta\sigma_T = \sigma_{ym} + \sqrt{\Delta\sigma_{LT}^2 + \Delta\sigma_{GR}^2 + \Delta\sigma_{OR}^2 + \Delta\sigma_{CTE}^2}\ . \tag{4}$$

The mechanism of load transfer is based on the transmission of the applied stress through the interface bond from the Al matrix to the graphene particles. For this reason, the graphene particles should be homogeneously distributed in the microstructure and have a strong bond of interface among the reinforcement and the matrix. Equation (5) explains this mechanism [42, 43]

$$\Delta\sigma_{LT} = (1/2)V_g\sigma_{ym}\ , \tag{5}$$

where V_g is the volumetric contribution of graphene and σ_{ym} is the yield strength of the aluminum. Grain refinement, achieved by GNPs located at grain boundaries, contributes to the enhanced strength of composites due to the resulting finer grain size. Graphene particles are homogeneously dispersed in the

microstructure and located at the grain boundaries, hence it inhibits grain size growth under the heat treatment process [44, 45]. The reduction in the grain size increases the material's yield strength ($\Delta\sigma_{GR}$). Hall-Petch equation (Equation (6)) explains the relationship with the strength and grain size of the material

$$\Delta\sigma_{GR} = \sigma_0 + K/\sqrt{d}\ , \tag{6}$$

where d is the particle size, K and σ_0 are the material constant. The mismatch in thermal expansion between graphene and aluminum generates internal stresses at the interface. These stresses increase the density of dislocations in the microstructure of the material. Therefore, the yield strength of the sample is enhanced [46]. Equation (7) can be used to calculate the rise in yield strength caused by thermal mismatch [47]

$$\Delta\sigma_{CTE} = KGb\sqrt{\rho_{CTE}}\ . \tag{7}$$

In this equation, G is the modulus of the shear of aluminum, b is the Burgers vector, ρ is the dislocation density, and K is a material constant. When dislocations formation during the plastic deformation encounters graphene particles, their movement is restricted or stopped. Dislocations bend around the graphene particles and form dislocation cycles. These cycles generate reverse stress that restricts their movement by acting as a blockade for dislocations in the same sliding plane. It causes the density of dislocations in the structure to increase [42, 48]. This condition, known as the Orowan mechanism, results in increased strength. The Orowan mechanism is expressed below [47]

$$\Delta\sigma_{OR} = (0.13bG\ /\ \lambda)\ ln\ (d/2b)\ , \tag{8}$$

where λ is the distance of the particles. GNPs in the microstructure act as an obstacle during dislocation movement. Additionally, graphene reinforcement leads to a decrease in the distance between particles. In the decreased interparticle distance, the dislocations are unable to bend sharply to pass between the particles [49]. Thus, shear stress is created in the structure to bending the dislocations. The influence of graphene content on particle spacing is described by Equation (9) [50]

$$\lambda = [4r(1-f)/3f]\ . \tag{9}$$

In this equation, r and f represent the radius of the graphene particles and the volume contribution of GNPs, respectively. As the distance between particles declines, the shear stress (τ_0) rises. This relation was expressed in Equation (10) [49]

$$\tau_0 = bG\ /\ \lambda\ . \tag{10}$$

4. RESULTS

In the present work, Al2024-GNPs, Al6061-GNPs, and Al7075-GNPs composites were produced by various heat treatment processes. The amount of graphene, matrix type and heat treatment process (sintering, hot pressing process) effects on mechanical properties, and microstructure were evaluated.

- The highest compressive strength (506±6 MPa) hardness (164±1.5 HV), and density (2.65 g/cm^3), were determined in sintered and hot-pressed Al7075-0.15%GNPs composites. However, the lowest porosity rate (4.4%) was obtained in Al6061-0.15%GNPs composites.
- In conclusion, Al7075 aluminum alloy showed the best mechanical properties among the matrix materials. Mechanical properties have been increased by the graphene reinforcement and it has been detected that graphene is an effective reinforcement element. In addition, hot pressing has a remarkable effect both on the microstructure and mechanical strength of the composites.
- Analyses of microstructure and mechanical test results showed that sintered and hot-pressed specimens exhibited a denser structure than only sintered samples. Because of the application of pressure and temperature at the same time in hot pressing, the intergranular distance decreased and the mechanical strength of the composite enhanced. Moreover, it did not cause any oxidation or deformation on the material surface, because this process is a fast and effective method. Since the

temperature control was done properly, the intergranular interaction increased in the microstructure of the samples exposed to high temperatures compared to the microstructure of only the sintered samples. Therefore, it has been determined that hot pressing processing improves the microstructure and mechanical strength of composite materials.

CONFLICTS OF INTEREST

No conflict of interest was declared by the authors.

REFERENCES

[1] Pul, M., "Effect of ZrO_2 quantity on mechanical properties of ZrO_2-reinforced aluminum composites produced by the vacuum infiltration technique", Revista de Metalurgia, 57(2): e195, (2021).

[2] Lawal, A.T., "Graphene-based nano composites and their applications: A review", Biosensors and Bioelectronics, 141: 111384, (2019).

[3] Ramanathan, A., Krishnan, P.K., and Muraliraja, R., "A review on the production of metal matrix composites through stir casting-furnace design, properties, challenges, and research opportunities", Journal of Manufacturing Processes, 42: 213–245, (2019).

[4] Zhao, Z., Bai, P., Du, W., Liu, B., Pan, D., Das, R., Liu, C., and Guo, Z., "An overview of graphene and its derivatives reinforced metal matrix composites: Preparation, properties and applications", Carbon, 170: 302–326, (2020).

[5] Tabandeh-Khorshid, M., Omrani, E., Menezes, P.L., and Rohatgi, P.K., "Tribological performance of self-lubricating aluminum matrix nanocomposites: Role of graphene nanoplatelets", Engineering Science and Technology, an International Journal, 19(1): 463–469, (2016).

[6] Gürbüz, M., "Atık içecek kutularından üretilmiş alüminyumun mekanik özelliklerine soğuk işlemin etkisi", Dokuz Eylül Üniversitesi Mühendislik Fakültesi Fen ve Mühendislik Dergisi, 20(58): 28–35, (2018).

[7] Samal, P., Vundavilli, P.R., Meher, A., and Mahapatra, M.M., "Recent progress in aluminum metal matrix composites: a review on processing, mechanical and wear properties", Journal of Manufacturing Processes, 59: 131–152, (2020).

[8] Aamir, M., Tolouei-Rad, M., Giasin, K., and Vafadar, A., "Machinability of Al2024, Al6061, and Al5083 alloys using multi-hole simultaneous drilling approach", Journal of Materials Research and Technology, 9(5): 10991–11002, (2020).

[9] Boppana, S.B., Dayanand, S., Anil Kumar, M.R., Kumar, V., and Aravinda, T., "Synthesis and characterization of ZrO_2 and graphene particle reinforced Al6061 metal matrix composites", In: Materials Today: Proceedings, 9(4): 7354–7362, (2020).

[10] Raghavendra, K., Shivaramakrishna, A., Basavaraj, Y., Sandeep, M.J., and Kumar, B.K.P., "Investigation on mechanical properties of Al7075 based MMC reinforced with Fe_3O_4", Materials Today: Proceedings, 66(4): 2080-2084, (2022).

[11] Al-Salihi, H.A., Mahmood, A.A., and Alalkawi, H.J., "Mechanical and wear behavior of AA7075 aluminum matrix composites reinforced by Al_2O_3 nanoparticles", Nanocomposites, 5(3): 67–73, (2019).

[12] Muralidharan, N., Chockalingam, K., Kalaiselvan, K., and Nithyavathy, N., "Investigation of ZrO_2 reinforced aluminium metal matrix composites by liquid metallurgy route", Advances in Materials and Processing Technologies, 9(2): 593-607, (2023).

[13] Navya, C., and Chandhrasekharareddy, M., "Development of aluminium based metal matrix composites by stir casting method", Materials Today: Proceedings, 68(5): 1685-1689, (2022).

[14] Dangarikar, S.U., and Dhokey, N.B., "Study of hot pressed sintering of premixed Al7075 based B_4C reinforced composites on wear mechanism", Materials Today: Proceedings, 44(6): 4749–4756, (2021).

[15] Scaria, C.T., Pugazhenthi, R., "Effect of process parameter on synthesizing of TiC reinforced Al7075 aluminium alloy nano composites", Materials Today: Proceedings, 37(2): 1978–1981, (2021).

[16] Surya, M.S., Prasanthi, G., "Manufacturing, microstructural and mechanical characterization of powder metallurgy processed Al7075/SiC metal matrix composite", Materials Today: Proceedings, 39(4): 1175–1179, (2021).

[17] Dinesh Kumar, S., Selvan, T.S., Sabariraj, R.V., Muthukumar, K., Elayaraja, D., and Greesan, R., "Studies on tribological behaviour of AA8050-Si_3N_4 composites", Materials Today: Proceedings, 74(1): 68-72, (2023).

[18] Moustafa, E.B., Melaibari, A., and Basha, M., "Wear and microhardness behaviors of AA7075/SiC-BN hybrid nanocomposite surfaces fabricated by friction stir processing", Ceramics International, 46(10): 16938–16943, (2020).

[19] Prakash, P.B., Raju, K.B., Venkatasubbaiah, K., and Manikandan, N., "Microstructure analysis and evaluation of mechanical properties of Al 7075 GNP's composites", Materials Today: Proceedings, 5(6): 14281–14291, (2018).

[20] Zhang, P.X., Jiang, Z., Zhang, C., and Guo, W., "Regulating microstructure, mechanical properties and electrochemical characteristic of 2024-CNTs aluminum composites via decorating nano Ni on the surface of CNTs", Diamond and Related Materials, 126: 1-13, (2022).

[21] Deaquino-Lara, R., Soltani, N., Bahrami, A., Gutiérrez-Castañeda, E., García-Sánchez, E., and Hernandez-Rodríguez, M.A.L.,"Tribological characterization of Al7075-graphite composites fabricated by mechanical alloying and hot extrusion", Materials and Design, 67: 224–231, (2015).

[22] Lee, X.J., Hiew, B.Y.Z., Lai, K.C., Lee, L.Y., Gan, S., Thangalazhy-Gopakumar, S., and Rigby, S., "Review on graphene and its derivatives: synthesis methods and potential industrial implementation", Journal of the Taiwan Institute of Chemical Engineers, 98: 163–180, (2019).

[23] Warner, J.H., Graphene: Fundamentals and Emergent Applications, Elsevier, UK, (2013).

[24] Darshan, M., Reddappa, H.N., Chandrashekar, A., and Vinod Kumar, R., "Mechanical and tribological properties of AA-7075 and graphene reinforced metal matrix composites", International Journal of Scientific Development and Research, 3(7): 230-235, (2018).

[25] Muraliraja, R., Aranachalam, R., Al-Fori, I., Al-Maharbi, M., and Piya, S., "Development of alumina reinforced aluminum metal matrix composite with enhanced compressive strength through squeeze casting process", Proceedings of the Institution of Mechanical Engineers, Part L: Journal of Materials: Design and Applications, 233(3): 307–314, (2018).

[26] Zamani, N.A.B.N., Asif Iqbal, A.K.M., Muhammad Nuruzzaman, D., "Fabrication and characterization of Al_2O_3 nanoparticle reinforced aluminium matrix composite via powder metallurgy", Materials Today: Proceedings, 29(1): 190–195, (2019).

[27] Haddad, A., Benamor, A., Chiker, N., Hadji, Y., Temmar, M., Hakem, M., Badji, R., Abdi, S., and Hadji, M., "Effect of heat treatment on microstructure and tribological behavior of friction stir processed Al_2O_3-reinforced AA2024-T351 matrix", International Journal of Advanced Manufacturing Technology, 115(5–6): 1671–1681, (2021).

[28] Veerappan, G., Abdi, D., Marichamy, S., Dhinakaran, V., and Sathish, S., "Investigation of mechanical properties and corrosion behavior of nickel bronze alloy prepared powder metallurgy", Materials Today: Proceedings, 74(1): 44-48, (2023).

[29] Chen, X., Zhu, R., Yuan, Z., Gao, H., Xu, W., Xiao, G., Xu, W., and Lu, Y., "Applied surface science in-situ construction of the nanostructured TiO_2/TiN composite films by induction heat treatment : improved mechanical, corrosion, and biological properties", Applied Surface Science, 614: 1-13, (2023).

[30] Fomin, A., Fomina, M., Koshuro, V., and Rodionov, I., "Composite metal oxide coatings on chromium-nickel stainless steel produced by induction heat treatment", Composite Structures, 229: 1-8, (2019).

[31] Chen, L., Qi, Y., Fei, Y., Liu, Y., and Du, Z., "GNP-reinforced Al2024 composite fabricated through powder semi-solid processing", Materials Transactions, 61(7): 1239–1246, (2020).

[32] Singh, P.K., "Mechanical characterization of graphene-aluminum nanocomposites", Materials Today: Proceedings, 44(1): 2304–2308, (2021).

[33] AbuShanab, W.S., Moustafa, E.B., Ghandourah, E., and Taha, M.A., "Effect of graphene nanoparticles on the physical and mechanical properties of the Al2024-graphene nanocomposites fabricated by powder metallurgy", Results in Physics, 19: 1-12, (2020).

[34] Kumar, P.G.H., and Xavior, A.M., "Effect of graphene addition on flexural properties of Al 6061 nanocomposites", Materials Today: Proceedings, 4(8): 8127–8133, (2017).

[35] Khan, M., Din, R.U., Wadood, A., Syed, W.H., Akhtar, S., and Aune, R.E., "Effect of graphene nanoplatelets on the physical and mechanical properties of Al6061 in fabricated and T6 thermal conditions", Journal of Alloys and Compounds, 790: 1076–1091, (2019).

[36] Chak, V., and Chattopadhyay, H., "Synthesis of graphene–aluminium matrix nanocomposites: mechanical and tribological properties", Materials Science and Technology, 37(5): 467–477, (2021).

[37] Xia, H.M., Zahng, L., Zhu, Y., Li, N., Sun, Y., Zhang, J., and Ma, H., "Mechanical properties of graphene nanoplatelets reinforced 7075 aluminum alloy composite fabricated by spark plasma sintering", International Journal of Minerals, Metallurgy and Materials, 27(9): 1295–1300, (2020).

[38] Şenel, M., and Üstün, M., "Dry sliding wear and friction behavior of graphene/ZrO_2 binary nanoparticles reinforced aluminum hybrid composites", Arabian Journal for Science and Engineering, 47(7): 9253–9269, (2022).

[39] Kumar, N., and Maheshwari, S., "Expounding the influence of micro/nano particles on mechanical and tribological properties of AA 7050 matrix composite: a review", Materials Today: Proceedings, 62(6): 3361–3367, (2022).

[40] Zhang, Z., and Chen, D.L., "Consideration of Orowan strengthening effect in particulate-reinforced metal matrix nanocomposites: A model for predicting their yield strength", 54(7): 1321–1326, (2006).

[41] Şenel, M., and Demir, M., "Effect of induction heat treatment on the mechanical propertiesof Si_3N_4–graphene-reinforced Al2024 hybrid composites", Bulletin of Materials Science, 45(1): 1–17, (2022).

[42] Chen, W., Yang, T., Dong, L., Elmasry, A., Song, J., Deng, N., Elmarakbi, A., Liu, T., Lu, H.B., and Fu, Y.Q., "Advances in graphene reinforced metal matrix nanocomposites: Mechanisms, processing, modelling, properties and applications", Nanotechnology and Precision Engineering, 3(4): 189–210, (2020).

[43] Luo, K., Liu, S., Xiong, H., Zhang,Y., Kon, C., and Yu, H., "Mechanical properties and strengthening mechanism of aluminum matrix composites reinforced by high-entropy alloy particles", Metals and Materials International, 28(11): 2811–2821, (2022).

[44] Ghodrati, H., and Ghomashchi, R., "Effect of graphene dispersion and interfacial bonding on the mechanical properties of metal matrix composites: an overview", FlatChem, 16: 1-22, (2019).

[45] Kang, Y.C., and Chan S.L., "Tensile properties of nanometric Al_2O_3 particulate-reinforced aluminum matrix composites", Materials Chemistry and Physics, 85(2–3): 438–443, (2004).

[46] Ma, P., Jia, Y., Gokuldoss, P.K., Yu, Z., Yang, S., Zhao, J., and Li, C., "Effect of Al_2O_3 nanoparticles as reinforcement on the tensile behavior of Al-12Si composites", Metals, 7(359): 1-11, (2017).

[47] Wang, F., Liu, H., Liu, Z., Guo, Z., and Sun, F., "Microstructure analysis, tribological correlation properties and strengthening mechanism of graphene reinforced aluminum matrix composites", Scientific Reports, 12(1): 1-11, (2022).

[48] Guler, O., and Bagci, N., "A short review on mechanical properties of graphene reinforced metal matrix composites", Journal of Materials Research and Technology, 9(3): 6808–6833, (2020).

[49] Dieter, G. E., Mechanical Metallurgy, McGraw Hill, New York, (1986).

[50] Latief, F.H., and Sherif, E.S.M., "Effects of sintering temperature and graphite addition on the mechanical properties of aluminum", Journal of Industrial and Engineering Chemistry, 18(6): 2129–2134, (2012).